Università Commerciale Luigi Bocconi

Master of Science in Data Science and Business Analytics

20599 Simulation and Modeling

Forecasting Arctic Shipping Routes Under Climate Change: A Network Approach

Target Journal

Transportation Research Part D: Transport and Environment

Group Members:

Jacopo Mattia D'Angelo, Luca Milani, Maximilian Rienth, Ioannis Thomopoulos

Professors and Teaching Assistants:

Dr Alessia Melegaro, Dr Lorenzo Lucchini, Duilio Balsamo

Declaration of Independence:

We declare that this report is the original work of the group members listed above and that all sources have been appropriately cited.

Academic Year 2024–2025

Contents

Abstract

This report evaluates how declining Arctic sea ice will affect the length and timing of trans-Arctic shipping routes between major Asian, European, and Atlantic shipping ports across varying risk thresholds. A simple linear ice-decay model based on 2015–2020 satellite data was developed and extended to 2050, which was subsequently turned into a lattice network. Using the A* algorithm on five ice-tolerance thresholds (15%, 22.5,%, 30%, 37.5%, 45% sea-ice concentration), daily least-cost paths for four corridors were created: Shanghai–New York, Shanghai–Rotterdam, Singapore–New York, and Singapore–Rotterdam. Model forecasts reproduce observed ice patterns with r = 0.924. Results show a steady increase in navigable days and a steady decrease in average route length across all thresholds. A sharp inflection occurs when annual navigable days reach about 150, coinciding with clearance of a key chokepoint: the *Bolshevik Strait*. High-tolerance vessels gain an abrupt 25–30 pixels ($\approx$ 625–750 km) distance advantage over low-tolerance vessels from this clearance. These findings demonstrate that vessel ice-tolerance not only governs when Arctic passages open but also how much distance savings operators can capture as sea ice retreats.

---

1 Introduction

Recent climate model projections suggest that the Arctic Ocean is likely to experience its first ice-free September as early as 2050, even under more optimistic scenarios where cumulative CO_2 emissions remain 1000 $GtCO_2$ below 2019 levels [1, 2]. The ongoing reduction in Arctic sea-ice area and thickness has expanded open-water areas and extended the duration of the melt season [1], creating new opportunities for maritime navigation [4].

As the navigable window expands, the tolerance of ships to residual ice becomes a key factor in determining how soon and how frequently emerging Arctic routes can be utilized. When considering non-specialized vessels, which can operate in open water with ice thickness up to 15 centimeters, studies project that by the end of the century, such vessels could traverse most of the Arctic for approximately six months each year. Although the exact duration varies by climate change scenario, projections consistently indicate that the potential for September transits through open water will at least double compared to historical conditions [5].

Although prior work has examined Arctic shipping through environmental, regulatory, and financial lenses [6, 7], most existing studies simulate Arctic maritime networks under static or scenario-based assumptions [8]. Consequently, this study aims to adopt a more dynamic approach by providing a threshold-sensitive view of when trans-Arctic shipping routes emerge. Previous graph-based simulations [9] are extended by coupling daily sea-ice forecasts with an A* path-finding algorithm to identify the shortest navigable maritime paths in a changing Arctic environment. Building on this approach, the study addresses the following research question:

"How does declining Arctic sea-ice concentration open new trans-Arctic shipping routes for vessels with different ice-risk tolerances?"

The analysis spans the 2025-2050 window, capturing the next quarter-century in which Arctic navigation prospects are expected to evolve most rapidly [2]. Moreover, we concentrate on four heavily trafficked Southeast-Asian to Atlantic corridors: *Shanghai–New York, Shanghai–Rotterdam, Singapore–New York, and Singapore–Rotterdam*, as these ports are to be the largest beneficiaries from the opening of Arctic routes [10, 11].

Route viability is evaluated across five ice-risk thresholds, which depend on the level of ice concentration the ships are able to pass through: 15%, 22.5%, 30%, 37.5% and 45%. These thresholds were selected based on historical data on shipping routes [12].

[1] The period, typically summertime, when above-freezing temperatures cause shrinking of Arctic sea ice[3]

2 Literature Review

2.1 Arctic Climate Change and Sea Ice Decline

Recent studies have shown that the Arctic is warming at nearly four times the global average, a process known as Arctic amplification [13, 14]. This warming has driven significant and persistent declines in both sea ice extent and thickness, expanded open water areas, and caused earlier spring snow melt and permafrost warming near the surface [13, 15].

Climate projections from CMIP6 models suggest that the Arctic could experience its first consistently ice-free September as early as 2035 under high-emission scenarios and as late as 2067 under low-emission scenarios. Under the most widely used scenarios framework, ice-free conditions are projected to occur around 2050. Spatially, sea ice loss is expected to begin in the European Arctic, progress through the Pacific Arctic, and eventually affect the central Arctic. Depending on the warming trajectory, ice-free periods may also extend into August and October [1, 16].

2.2 Sea Ice Forecasting

The primary objective of this study is to evaluate the future navigability of Arctic shipping routes by forecasting sea-ice concentration, the key determinant of when and where vessels can transit through these waters. This metric was chosen due to its dominant influence on navigation feasibility [17, 18]. Although latest climate models, such as those in CMIP6, aim to simulate ice dynamics with high-resolution configurations, they often fall short in capturing the nuances required for regional-scale navigability assessments. For example, the MPI-ESM-1-2-HR model, which offers high spatial resolution and advanced ice dynamics, remains computationally expensive and still exhibits notable biases, such as the overestimation of sea-ice extent during the September minimum and difficulty in accurately representing thick ice sea within the Canadian Arctic Archipelago [19]. Given these limitations and the fact that high-resolution climate modeling is not the central focus of this research, a simpler, empirical forecasting strategy has been adopted. A trend-based model was constructed using recent observational data. Specifically, a uniform linear decay was applied to a baseline seasonal cycle beginning on 15 September 2025 and continuing through 15 September 2050 [1, 2]. This approach maintains the observed historical seasonal cycle while gradually reducing sea-ice coverage over time. This approach yields an easily interpretable projection of sea-ice retreat, while avoiding the risk of misleading details that climate models may introduce [20]. The slope of this decay was chosen to be consistent with mid-century projections indicating that the Arctic will be ice-free in September by around 2050 under all emission scenarios [1]. Although this approach does not attempt to model internal ice dynamics in detail, it offers a pragmatic balance between realism and computational efficiency.

2.3 Modeling Frameworks

This study utilizes the A* algorithm to assess navigability and determine the shortest traversable distance across four major routes. Unlike Breadth First Search, the A* algorithm operates on weighted graphs, enabling more realistic modeling of path costs. Although recent research on Arctic shipping routes has primarily employed Dijkstra's algorithm to identify paths with minimal navigation risk [9, 21], A* offers a notable computational advantage. Specifically, A* incorporates a heuristic function (Euclidean distance) to estimate the remaining cost to the goal. This allows A* to prioritize promising paths and reduce the number of nodes explored, whereas Dijkstra's algorithm blindly explores all directions based on the smallest tentative distances. In terms of asymptotic complexity, both algorithms are theoretically equivalent. Dijkstra's algorithm exhibits a time complexity of $\Theta(n^2)$, where n is the number of nodes. The A* algorithm has a time complexity of $\Theta(m \times n)$, where $0 \leq m \leq n$, depending on the number of nodes evaluated based on the heuristic. However, in practice, A* often achieves faster performance due to its heuristic-driven search strategy [22].

2.4 Arctic Shipping Routes

The Arctic Passage connects the North Pacific and North Atlantic via three primary routes:

- **Northern Sea Route (NSR):** Runs along Russia's northern coast, linking Europe and Asia. It can reduce transit distance by roughly one-third compared to the Suez Canal depending on departure and arrival ports [23].
- **Northwest Passage (NWP):** Passes through the Canadian Arctic Archipelago. While simulations show potential for faster transit and round-trip efficiency compared to the Panama Canal [24], it remains constrained by ice, geography, and limited infrastructure [25].
- **Transpolar Sea Route (TSR):** Crosses the central Arctic Ocean near the North Pole, offering the shortest possible link between the Pacific and Atlantic Oceans. This route is currently not available but it is expected to become seasonally navigable by mid-century, contingent on emissions scenarios [25].

In terms of accessibility to these routes, they can be deemed 'ice-free' at 15% sea-ice coverage and less, as per the National Snow and Ice Data Center (NSIDC) definition of ice-free [26]. Thus, this was used as the lowest threshold in the study with higher thresholds being chosen starting from this baseline. Furthermore, a 45% threshold was used as the ceiling since at this point it becomes 'difficult' to navigate [12].

2.5 Economic and Geopolitical Considerations

As Arctic sea-ice decline opens new maritime corridors, the implications extend well beyond navigational efficiency. Trans-Arctic shipping is poised to reshape global maritime trade dynamics, with the Northern Sea Route (NSR) currently offering the most immediate commercial potential. Studies suggest that the NSR could reduce travel distances by up to 40% [27] and lower shipping costs between Asia and Europe by 10–20% compared to traditional routes via the Suez Canal [28]. In contrast, the Transpolar Sea Route (TSR) remains largely theoretical but promises the most direct link between the Atlantic and Pacific Oceans, bypassing both the Suez and Panama Canals entirely [25]. Although not yet viable, the TSR is increasingly viewed as a long-term strategic asset [6].

These economic prospects have not gone unnoticed by Arctic and non-Arctic states, which are intensifying competition over access, jurisdiction, and control of emerging sea routes. Canada claims that the Northwest Passage constitutes internal waters under its sovereignty [29], while Russia exerts de facto authority over the NSR, imposing domestic regulations that challenge international norms such as freedom of navigation [6]. The United States has responded by launching inquiries into the NSR's strategic significance as a global maritime chokepoint [30, 31]. Meanwhile, China, which identifies itself as a "near-arctic state", has framed the TSR as a core component of its Polar Silk Road initiative, accelerating investments in Arctic infrastructure and scientific research to secure future access [32]. Legal ambiguities continue to surround the TSR, particularly regarding the application of the United Nations Convention on the Law of the Sea (UNCLOS) to issues of navigational rights and exclusive economic zones [33].

3 Methods

3.1 Data Sources

Daily sea-ice concentration satellite rasters (GeoTIFF - Pixel resolution: 25 km x 25 km) were taken from the NSIDC Sea-Ice Concentration Climate Data Record, Version 3 for the period spanning 2015 to march 2025 [34]. A static land–water mask of the northern hemisphere is taken from the Natural Earth "Raster Land and Ocean" medium-scale dataset (v5.1) [35]. These two layers are merged to form the input stack for all subsequent preprocessing and routing steps.

3.2 Ice Forecasting Pipeline

3.2.1 Data Preprocessing

The daily Arctic GeoTIFF rasters from 2015 through 2020 each encode the sea-ice concentration in the following scale:

$$C_{y,d}(i,j) \in [0,1000]$$

for day d of year y at grid cell (i,j). Leap days (February 29) are omitted. All rasters are processed in their native projection and resolution. Grid cells that remained `nodata` throughout the 6-year window were excluded from all modeling. Additionally, we defined two fixed pixel masks:

$$\begin{aligned} \text{land pixels:} \quad & \max_{y,d} C_{y,d}(i,j) > 2000, \\ \text{water pixels:} \quad & \max_{y,d} C_{y,d}(i,j) \leq 10, \end{aligned}$$

which are assumed to remain unchanged throughout the forecast.

3.2.2 Baseline Seasonal Cycle

To capture the mean seasonal cycle, a climatological baseline was computed for each calendar day $d \in \{1,\ldots,365\}$ by averaging across available years:

$$\overline{C}(d) \;=\; \frac{1}{N_d} \sum_{y=2015}^{2020} \big\langle C_{y,d}(i,j) \big\rangle_{i,j}, \tag{1}$$

where $\langle \cdot \rangle_{i,j}$ denotes a spatial average over non-masked pixels, and N_d is the number of valid years contributing to day d.

3.2.3 Linear Ice Decay Model

To simulate long-term decline, an assumption of linear decay was used between:

$$t_0 = \text{2024-09-15}, \quad t_{\text{end}} = \text{2050-09-15}.$$

The decay multiplier was defined as:

$$M(t) = \begin{cases} 1, & t < t_0, \\ 1 - \dfrac{t - t_0}{t_{\text{end}} - t_0}, & t_0 \leq t \leq t_{\text{end}}, \\ 0, & t > t_{\text{end}}. \end{cases} \tag{2}$$

While more sophisticated models could improve accuracy, the focus was on estimating navigability, not exact ice dynamics. The linear formulation balanced simplicity with seasonally grounded behavior.

3.2.4 Forecast Generation

For each date t from 2025-01-01 to 2050-12-31, the day-of-year index $d(t) \in \{1,\ldots,365\}$ was computed (excluding leap days). The forecast was defined as:

$$\widehat{C}(t) \;=\; M(t) \;\times\; \overline{C}\big(d(t)\big). \tag{3}$$

This ensured seasonal structure (via Eq. 1) while enforcing a long-term decline (via Eq. 2). The result was a forecasted raster for each day from 2025 through 2050. The zero-ice date of 15 September 2050 was selected based on projections from the literature [1, 2].

3.3 Routing Algorithm and Network Modeling

3.3.1 Route Selection and Objectives

The shortest navigable routes for four major port pairs were modeled: *Shanghai–New York, Shanghai–Rotterdam, Singapore–New York, and Singapore–Rotterdam.* These routes were selected to capture strategic global trade flows and interactions with traditional canals (Suez and Panama).

3.3.2 Routing Grid Construction

Each daily forecasted raster is re-projected to the polar stereographic north projection (EPSG:3411) for visibility. Grid cells are treated as traversable if:

$$C < \text{Threshold}, \quad \text{where Threshold} \in \{150, 225, 300, 375, 450\}^{2}.$$

These threshold values were used to represent a spread of vessel ice navigability that is in line with the literature, which states that approximately 70% of vessels can navigate at the 300 threshold [36]. Land pixels (value = 3000), and sea ice above the chosen threshold are treated as impassable.

3.3.3 Lattice Representation of the Grid

Each reprojected sea-ice raster is treated as a lattice in which each pixel becomes a node (i, j). This lattice framework allows the ice concentration field to be interpreted as a weighted graph ($\approx 975{,}000$ nodes), with the pixel values mentioned above as weights. Nodes are connected under a Moore neighbourhood [37], allowing movement to any of the eight surrounding cells. Nodes with ice concentration below the defined thresholds are assigned dynamic traversal costs proportional to their concentration values, while land and ice cells above the threshold C are treated as impassable barriers. This lattice network is the base structure for the A* pathfinding algorithm, enabling the identification of daily least-cost paths for each route.

3.3.4 Canal Integration

To ensure connectivity across hemispheres, channels were manually carved along the Suez and Panama canals using known geospatial paths (as they are too small to appear at the resolution of the satellite data). Edge weights (pixel values) in these areas were forcibly set to zero in the lattice.

3.3.5 A* Algorithm Implementation

The A* search algorithm is applied on each daily ice raster to compute the least-cost path from source ports to target ports. The cost function combines path length and ice concentration:

$$f(i, j) = G(i, j) + h(i, j),$$

where $G(i, j)$ is the accumulated cost to reach cell (i, j), and $h(i, j)$ is the Euclidean distance to the goal. Each step has cost:

$$\text{step\_cost} = d \cdot \left(1 + \frac{C(i, j)}{1000}\right),$$

with $d \in \{1, \sqrt{2}\}$ depending on move direction (cardinal vs. diagonal). Since the Euclidean heuristic never exceeds the minimum remaining travel cost, it is admissible, and A* therefore guarantees an optimal least-cost path for every day and ice-risk threshold.

3.4 Termination Criteria

To reduce computation while still capturing navigability windows, a two-pass strategy was for each year (2025–2050):

- **Forward pass:** September → December
- **Backward pass:** August → January

Each pass stopped early when, for seven consecutive days, every calculated path had a distance indicating that the A* algorithm had defaulted to the traditional Suez or Panama Canal routes, showing that extending the simulation into the deeper winter months would add computation without revealing any additional navigable days.

[2] In the text we use ice concentration C in its percentage equivalent (e.g. 150 denotes 15 % ice cover).

4 Results

4.1 Verifying Arctic Route

The two panels below compare optimal shipping paths in January (left) and August (right) for the same origin-destination pairs in 2025 (see Figure 1). In January, the Arctic is locked in thick ice, so the A* shortest-path algorithm routes vessels along the traditional canals paths (Panama or Suez), despite their longer distance as the Arctic ice is 'impenetrable'. By August, however, sea-ice retreat opening a trans-Arctic corridor over northern Russia. Showing that when the Arctic ice clears beyond each vessel's ice tolerance, the algorithm switches to the Arctic route because it cuts hundreds of kilometers off the voyage compared to the traditional canal alternatives. This dynamic behavior shows how, as summer ice thins, ships can exploit the true shortest path over the pole rather than follow the longer, fixed traditional waterways.

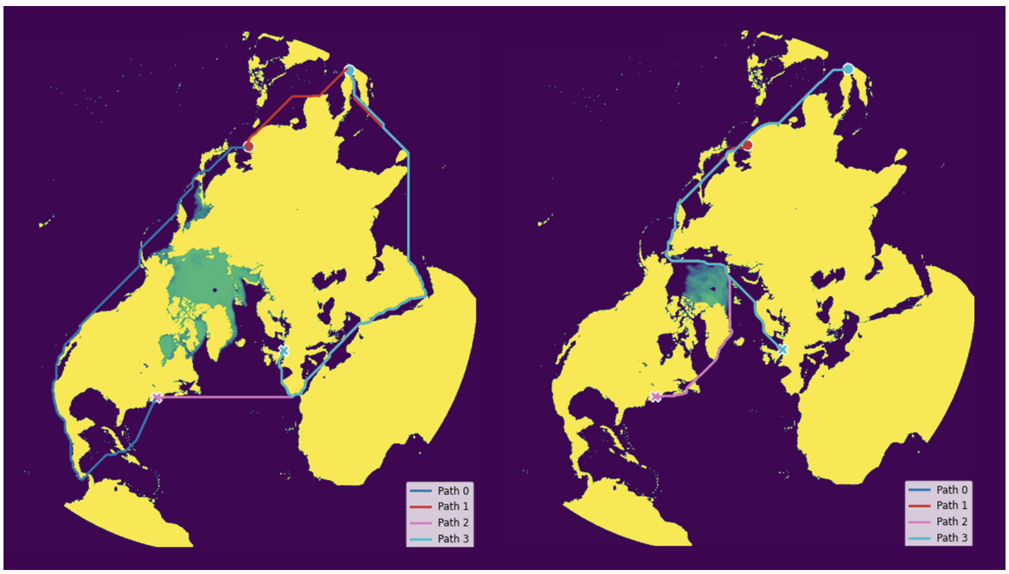

Figure 1: January vs August 2025 Routes

4.2 Average Route Distance per Threshold

Figure 2 plots the mean route length aggregated across all four routes under the five ice-concentration thresholds, from 2025 to 2045. As expected, all curves slope downward, indicating that average route length steadily decreases as Arctic sea ice retreats. More importantly, the vertical spacing between the threshold curves quantifies how much risk tolerance reduces voyage distance.

In the early 2030s, the 450 threshold route is on average 15-20 pixels shorter than the 150 route. By the mid-2040s, this gap grows to nearly 65 pixels, even as all routes continue to shorten. Each threshold increase consistently translates into roughly 5-10 pixels of distance savings at key inflection points.

A notable pattern is the two-phase trajectory of the higher-tolerance routes: their lengths stall until roughly 2034, and then plunge much more rapidly in the period after. In contrast, the 15 % curve declines almost steadily, shaving a few pixels each year as peripheral ice melts. These contrasting slope patterns merit closer investigation in the following section.

4.3 Navigable Days per Threshold

To understand what drives these peculiar route patterns, the navigable days per year of the Arctic routes across thresholds are analyzed (see Figure 3).

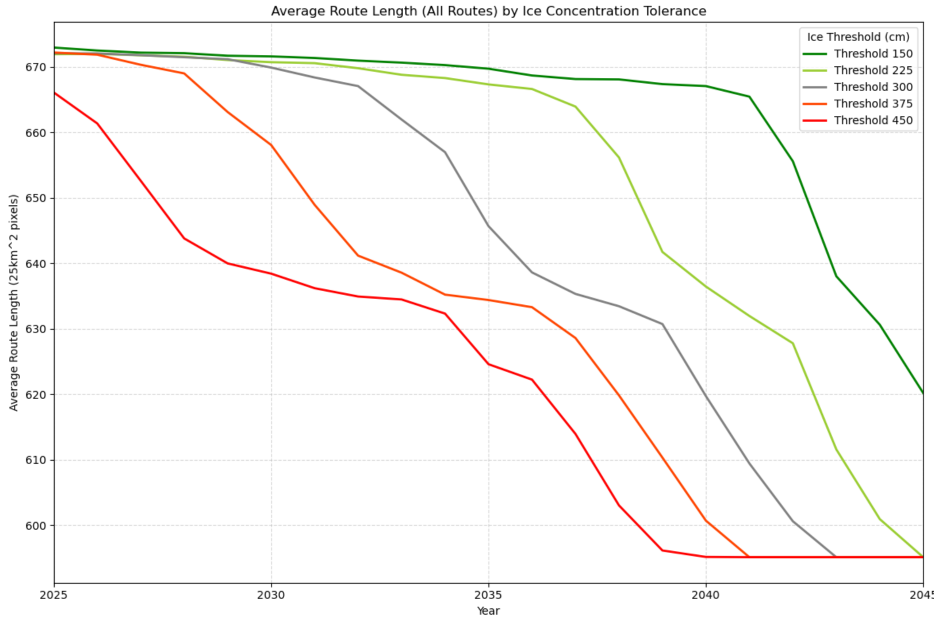

Figure 2: Average Route Length (All Routes) by Ice Concentration Tolerance (2025–2045).

The analysis reveals a consistent threshold behavior that matches the two-phase trajectory observed above. For each threshold, navigable days increase steadily until approximately 150 days per year, after which there is a rapid expansion of navigable days across all thresholds.

When that milestone is reached (about 2034 for the 37.5% 45% thresholds), a key corridor clears and their average travel distance drops in one sharp step. Before that point, their routes stay long and change very little. Lower-tolerance vessels need several more years to reach the same 150-day window, so their distances shrink slowly and steadily rather than all at once. This abrupt increase, or "elbow," suggests the year-round opening of a specific choke-point for full trans-Arctic connectivity.

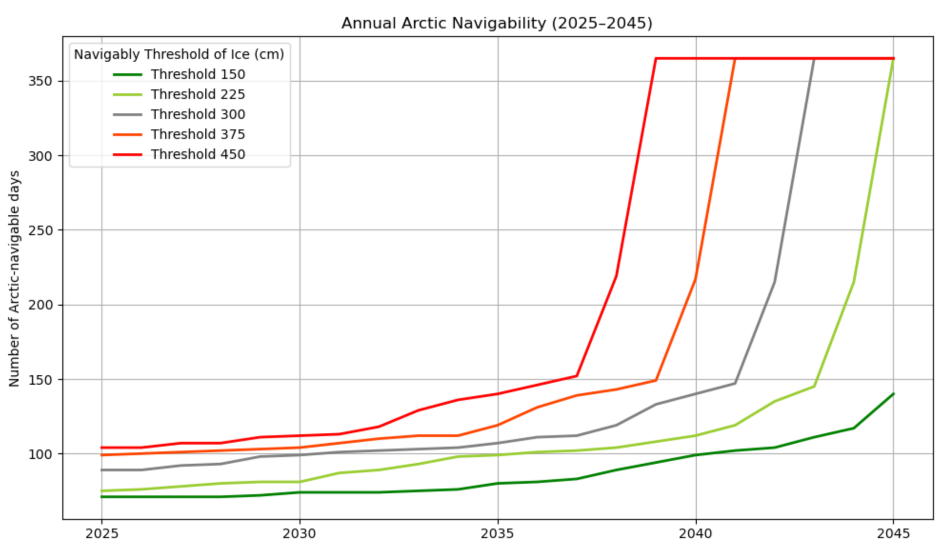

Figure 3: Annual number of Arctic-navigable days (2025–2045) for different ice concentration thresholds.

4.4 Regional Holdout Investigation

To pinpoint the regional choke-point, we compared the set of newly navigable cells on the day the corridor first opened with those from three days before the opening. These newly navigable cells are coloured in red in Figure 4.

This region was identified as the *Bolshevik Strait*. This strait lies along the Northern Sea Route between mainland Russia and Bolshevik Island. Once this strait becomes navigable, the Arctic shipping routes open entirely. Consequently, the ice conditions around the northern side of Bolshevik Island effectively delay the full navigability of these Arctic passages, underscoring the strategic significance of this region in future maritime Arctic operations.

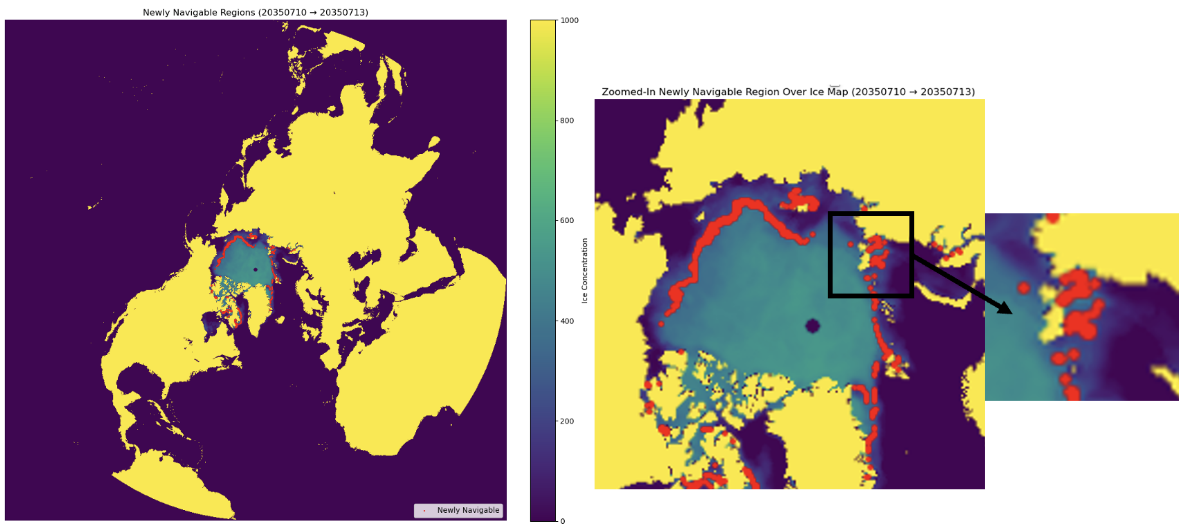

Figure 4: Newly navigable water between 2035-07-10 & 2035-07-13, highlighting the Bolshevik Strait.

5 Evaluation & Limitations

5.1 Evaluation

To assess the validity of the forecasted Arctic navigability, model predictions were compared to actual ice concentration data for 2025 obtained from the NSIDC database. The model achieved a strong Pearson correclation coefficient with an r-value of 0.924, indicating that the general spatial patterns and seasonality of ice concentration were captured effectively.

5.2 Limitations

Despite the robust routing framework and comprehensive historical baseline, several limitations should be noted:

- **Simplistic Decay Model:** The ice decay model assumes a linear decline to zero ice by 2050, which oversimplifies the complex interplay of climate variability, local oceanography, and atmospheric dynamics that influence ice concentration.
- **Fixed Threshold Analysis:** While multiple thresholds were explored, they do not fully capture the nuanced risk tolerances of different vessel types and operational strategies in ice-infested waters.
- **Spatial Resolution Constraints:** The analysis relies on the native resolution of the ice concentration rasters, potentially overlooking finer-scale navigability details relevant to specific vessel sizes and route planning.

- **Geopolitical and Infrastructural Factors:** Non-physical constraints such as shipping regulations, port readiness, and Geo-Political issues, were not incorporated, even though they are critical for real-world route viability.

5.3 Future Work

Future improvements could include integrating higher-resolution ice forecasting models, incorporating climate variability scenarios beyond linear trends, and combining ice concentration with vessel-specific risk assessments. Further, expanding the analysis to include seasonal and inter-annual variability would provide a more nuanced understanding of the evolving Arctic shipping landscape.

6 Conclusion

This study has demonstrated the increasing viability of future Arctic shipping routes across varying risk thresholds. Through a data-driven framework combining historical ice concentration data, a linear decay projection model, and dynamic routing via the A* algorithm, we have quantified the trade-off between route length and risk tolerance, the number of navigable days for key trans-Arctic trade corridors, as well as the identification of a key hold-up region and the subsequent impact of when this hold-up region is avoided.

The analysis revealed a critical inflection point, around 150 annual navigable days, marking the opening of a maritime bottleneck. Specifically, the *Bolshevik Strait*, along the Northern Sea Route, emerged as the holdout region whose clearance enables year-round trans-Arctic passage.

Comparing across ice thresholds showed that vessels with greater ice navigation capability (higher thresholds) will access Arctic routes significantly earlier, demonstrating the importance of vessel-specific ice tolerances in route planning. Lower thresholds, although more conservative, still exhibit a clear trend of expanding accessibility over the forecast period, albeit delayed by nearly a decade compared to the highest thresholds.

These findings have clear implications for stakeholders in Arctic maritime trade. The steady increase in navigable days, combined with the sudden accessibility surge once key regional bottlenecks clear, suggests that strategic monitoring of these choke-points is critical. Since access swings from seasonal to year-round in a very short span, operators cannot count on a gradual learning curve; ice-class vessels, trained crews, insurance cover, and port support must be in place before the choke-point opens.

Additionally, as the Bolshevik Strait is located within Russian territorial waters, Russia exercises effective control over its use, paralleling its broader regulatory stance along the Northern Sea Route [6]. This control introduces an important layer of operational uncertainty for international shipping operators, who must navigate not only environmental barriers but also regulatory, economic, and political considerations shaped by Russian governance.

Overall, this study contributes to the understanding of how sea ice decline is reshaping Arctic navigability at varying risk tolerances, offering a framework that combines climate data, spatial analysis, and routing algorithms to inform both commercial and policy considerations for the region's evolving maritime landscape.

References

[1] D. Notz and SIMIP Community. Arctic sea ice in cmip6. *Geophysical Research Letters*, 47(10), 2020. Accessed May 6, 2025.

[2] ESA Climate Office. Simulations suggest ice-free arctic summers by 2050, 2020. Accessed May 6, 2025.

[3] Abigail Smith and Alexandra Jahn. Definition differences and internal variability affect the simulated arctic sea ice melt season. *The Cryosphere*, 13(1):1–20, 2019.

[4] K. R. Barnhart and et al. Mapping the future expansion of arctic open water. *Nature Climate Change*, 6(3):280–285, 2015. Accessed May 6, 2025.

[5] Alex Crawford, Julienne Stroeve, Anna Smith, et al. Arctic open-water periods are projected to lengthen dramatically by 2100. *Communications Earth & Environment*, 2:109, 2021.

[6] Adolf K.Y. Ng, Andreas Becker, Scott Cahoon, Shuo Chen, Peter Earl, Sean Earl, and Zaili Yang. Implications of climate change for shipping: Opening the arctic seas. *Wiley Interdisciplinary Reviews: Climate Change*, 9(2), 2018. Accessed May 6, 2025.

[7] Frédéric Lasserre. Arctic shipping: A contrasted expansion of a largely destinational market. In Sebastian Knecht and Kathrin Keil, editors, *Commercial and Scientific Uses of the Northern Sea Route*, pages 85–103. Springer, 2018.

[8] J. Guo, S. Guo, and J. Lv. Potential spatial effects of opening arctic shipping routes on the shipping network of ports between china and europe. *Marine Policy*, 136:104885, 2022. Accessed May 6, 2025.

[9] S. Wang and et al. Projected navigability of arctic shipping routes based on climate model fio-esm v2.1. *Anthropocene*, 47:100445, 2024. Accessed May 6, 2025.

[10] Hua Xu, Zhifang Yin, Dashan Jia, Fengjun Jin, and Hua Ouyang. The potential seasonal alternative of asia–europe container service via northern sea route under the arctic sea ice retreat. *Maritime Policy & Management*, 38(5):541–560, 2011.

[11] Yiru Zhang, Qiang Meng, and Szu Hui Ng. Shipping efficiency comparison between northern sea route and the conventional asia-europe shipping route via suez canal. *Journal of Transport Geography*, 57:241–249, 2016.

[12] Hiroki Shibata, Koh Izumiyama, Kazutaka Tateyama, Hiroyuki Enomoto, and Shuhei Takahashi. Sea-ice coverage variability on the northern sea routes, 1980–2011. *Annals of Glaciology*, 54(62):139–148, 2013.

[13] M. Rantanen, A. Y. Karpechko, A. Lipponen, K. Nordling, O. Hyvärinen, K. Ruosteenoja, T. Vihma, and A. Laaksonen. The arctic has warmed nearly four times faster than the globe since 1979. *Communications Earth Environment*, 2022. Accessed May 6, 2025.

[14] M. C. Serreze and R. G. Barry. Perspectives on the arctic amplification of climate change. *Global and Planetary Change*, 2011. Accessed May 6, 2025.

[15] Jason E. Box, William T. Colgan, Torben Røjle Christensen, Niels Martin Schmidt, Magnus Lund, Frans-Jan W. Parmentier, Ross Brown, Uma S. Bhatt, Eugénie S. Euskirchen, Vladimir E. Romanovsky, John E. Walsh, James E. Overland, Muyin Wang, Robert W. Corell, Walter N. Meier, Bert Wouters, Sebastian Mernild, Johanna Mård, Janet Pawlak, and Morten Skovgård Olsen. Key indicators of arctic climate change: 1971–2017. *Environmental Research Letters*, 14(4):045010, 2019. Accessed May 6, 2025.

[16] Alexandra Jahn, Marika M. Holland, and Jennifer E. Kay. Projections of an ice-free arctic ocean. *Nature Reviews Earth & Environment*, 5:164–176, 2024. Accessed May 6, 2025.

[17] Rajesh Kandel and Hiba Baroud. A data-driven risk assessment of arctic maritime incidents: Using machine learning to predict incident types and identify risk factors. *Reliability Engineering System Safety*, 243:109779, 2024.

[18] X. Yang, Z.Y. Lin, W.J. Zhang, S. Xu, M.Y. Zhang, Z.D. Wu, and B. Han. Review of risk assessment for navigational safety and supported decisions in arctic waters. *Ocean Coastal Management*, 247:106931, 2024.

[19] Martin Henke, Felício Cassalho, Tyler Miesse, Celso M. Ferreira, Jinlun Zhang, and Thomas M. Ravens and. Assessment of arctic sea ice and surface climate conditions in nine cmip6 climate models. *Arctic, Antarctic, and Alpine Research*, 55(1):2271592, 2023.

[20] A. J. Cook, J. Dawson, S. E. L. Howell, et al. Sea ice choke points reduce the length of the shipping season in the northwest passage. *Communications Earth & Environment*, 5:362, 2024.

[21] *A Dynamics-Constrained Rapid Path-Planning Method for Shipping in Arctic Waters*, volume All Days of *International Ocean and Polar Engineering Conference*, 06 2024.

[22] A. Candra, M.A. Budiman, and K. Hartanto. Dijkstra's and a-star in finding the shortest path: A tutorial. In *2020 International Conference on Data Science, Artificial Intelligence, and Business Analytics (DATABIA)*, 2020. Accessed May 6, 2025.

[23] Eddy Bekkers, Joseph F. Francois, and Hugo Rojas-Romagosa. Melting ice caps and the economic impact of opening the northern sea route. *The Economic Journal*, 128(610):1095–1127, 2018. Accessed May 6, 2025.

[24] Dongqin Lu, Gyei-Kark Park, Kyounghoon Choi, and Sangjin Oh. An economic analysis of container shipping through canadian northwest passage. *International Journal of e-Navigation and Maritime Economy*, 1:60–72, 2014. Accessed May 7, 2025.

[25] Yu Zhang, Xiaopeng Sun, Yufan Zha, Kun Wang, and Changsheng Chen. Changing arctic northern sea route and transpolar sea route: A prediction of route changes and navigation potential before mid-21st century. *Journal of Marine Science and Engineering*, 11(12):2340, 2023. Accessed May 6, 2025.

[26] National Snow and Ice Data Center. About sea ice data and analysis tools. https://nsidc.org/sea-ice-today/about-data, 2025. Accessed May 25, 2025.

[27] Miaojia Liu and Jacob Kronbak. The potential economic viability of using the northern sea route (nsr) as an alternative route between asia and europe. *Journal of Transport Geography*, 18(3):434–444, 2010. Tourism and climate change.

[28] Frédéric Lasserre. Case studies of shipping along arctic routes. analysis and profitability perspectives for the container sector. *Transportation Research Part A: Policy and Practice*, 66:144–161, 2014.

[29] P. Whitney Lackenbauer and Adam Lajeunesse. On uncertain ice: The future of arctic shipping and the northwest passage, 2014. ISBN: 978-1-927573-18-1.

[30] Federal Maritime Commission. Fmc launching examination of global maritime chokepoints, 2025. Accessed: 07 May 2025.

[31] Malte Humpert. Us government investigates strategic importance of northern sea route as part of study on maritime chokepoints. *High North News*, 2025. Accessed: 07 May 2025.

[32] Ashton Basak. The arctic trilemma: The united states must compete for the transpolar sea route, October 2024. Accessed: 07 May 2025.

[33] Mia M. Bennett, Scott R. Stephenson, Kang Yang, Michael T. Bravo, and Bert De Jonghe. The opening of the transpolar sea route: Logistical, geopolitical, environmental, and socioeconomic impacts. *Marine Policy*, 121:104178, 2020. Accessed May 7, 2025.

[34] Florence Fetterer, Kristina Knowles, Walter N. Meier, Mark Savoie, and Alexandra K. Windnagel. Sea ice index, version 3. https://doi.org/10.7265/N5K072F8, 2017. [Data set] Accessed: 2025-05-28. Describe subset used if applicable.

[35] Natural earth: Free vector and raster map data at 1:10m, 1:50m, and 1:110m scales. https://www.naturalearthdata.com/downloads/, 2025. Public Domain. Made with Natural Earth.

[36] Yaqing Shu, Hailong Cui, Lan Song, Langxiong Gan, Sheng Xu, Jie Wu, and Chunmiao Zheng. Influence of sea ice on ship routes and speed along the arctic northeast passage. *Ocean & Coastal Management*, 256:107320, 2024. Accessed May 6, 2025.

[37] Chi-Ying Huang, Chuen-Tsai Sun, Jui-Lin Hsieh, Yi-Min Chen, and Hsien-Tang Lin. A novel small-world model: Using social mirror identities for epidemic simulations. *Simulation*, 81(9):671–699, 2005.